Available online at www.sciencedirect.com

ScienceDirect

Nuclear Physics B 915 (2017) 10–18

NUCLEAR PHYSICS B

www.elsevier.com/locate/nuclphysb

Axionic dark matter signatures in various halo models

J.D. Vergados [a,b,c,*,1], Y.K. Semertzidis [a,b]

[a] *Center for Axion and Precision Physics Research, Institute for Basic Science (IBS), Daejeon 34141, Republic of Korea*
[b] *Department of Physics, Korea Advanced Institute of Science and Technology (KAIST), Daejeon 34141, Republic of Korea*
[c] *ARC Centre of Excellence in Particle Physics at the Terascale and Centre for the Subatomic Structure of Matter (CSSM), University of Adelaide, Adelaide SA 5005, Australia*

Received 5 February 2016; received in revised form 23 November 2016; accepted 4 December 2016

Available online 6 December 2016

Editor: Hong-Jian He

Abstract

In the present work we study possible signatures in the Axion Dark Matter searches. We focus on the dependence of the expected width in resonant cavities for various popular halo models, leading to standard velocity distributions, e.g. Maxwell–Boltzmann, as well as phase-mixed and non-virialized axionic dark matter (flows, caustic rings). We study, in particular, the time dependence of the resonance width (modulation) arising from such models. We find that the difference between the maximum (in June) and the minimum (in December) can vary by about 10% in the case of standard halos. In the case of mixed phase halos the variation is a bit bigger and for caustic rings the maximum is expected to occur a bit later. Experimentally such a modulation is observable with present technology.

1. Introduction

The axion has been proposed a long time ago as a solution to the strong CP problem [1] resulting to a pseudo Goldstone Boson [2,3]. Its importance to Cosmology has also been recognized [4–6] long time ago and a bit later it has been considered as a prominent dark matter

* Corresponding author.
E-mail address: vergados@uoi.gr (J.D. Vergados).
[1] On leave: Physics Department, University of Ioannina, Greece.

http://dx.doi.org/10.1016/j.nuclphysb.2016.12.002

candidate [7]. In fact, realizing an idea proposed a long time ago by Sikivie [8], various experiments such as ADMX and ADMX-HF collaborations [9–12] are now planned to search for them, using SQUID and HFET technologies [13]. In addition, the newly established center for axion and physics research (CAPP) has started an ambitious axion dark matter research program [14], using high volume geometry and high field magnet technology. The allowed parameter space [15], containing information for all the axion like particles, defines a region for invisible axions, which can be dark matter candidates.

In the present work we will assume that the axion is non-relativistic with mass in μeV–meV scale, moving with an average velocity which is $\approx 0.8 \times 10^{-3}$ c. It is expected to be observed in resonance cavities with a width that depends on the axion mean square velocity in the local frame. The latter depends on the assumed halo model. We will expand and improve our previous work [16,17] by including various popular halo models. We will study the time variation of the width due to the motion of the Earth around the sun and the motion of the sun around the center of the galaxy, an important signature needed if indeed the predicted axion to photon coupling becomes weaker as some recent models predict [18].

2. Brief summary of the formalism

The photon axion interaction is dictated by the Lagrangian:

$$\mathcal{L}_{a\gamma\gamma} = g_{a\gamma\gamma} a \mathbf{E} \cdot \mathbf{B}, \; g_{a\gamma\gamma} = \frac{\alpha g_\gamma}{2\pi f_a}, \tag{2.1}$$

where $\mathbf{E}$ and $\mathbf{B}$ are the electric and magnetic fields, g_γ a model dependent constant of order one [9,19,20] and f_a the axion decay constant. Axion dark matter detectors [19] employ an external magnetic field, $\mathbf{B} \to \mathbf{B}_0$ in the previous equation, in which case one of the photons is replaced by a virtual photon, while the other maintains the energy of the axion, which is its mass plus a small fraction of kinetic energy.
The power produced, see e.g. [9], is given by:

$$P_{mnp} = g_{a\gamma\gamma}^2 \frac{\rho_a}{m_a} B_0^2 V C_{mnp} Q_L \tag{2.2}$$

Q_L is the loaded quality factor of the cavity. Here we have assumed Q_L is smaller than the axion width Q_a, see below. More generally, Q_L should be substituted by min (Q_L, Q_a). This power depends primarily on the axion density, but, as we shall see, the width of the expected resonance depends on the assumed velocity distribution.

The axion power spectrum [19,21], which is of great interest to experiments, is written as a Breit–Wigner shape [19]:

$$|\mathcal{A}(\omega)|^2 = \frac{\rho_D}{m_a^2} \frac{\Gamma}{(\omega - \omega_a)^2 + (\Gamma/2)^2}, \Gamma = \frac{\omega_a}{Q_a} \tag{2.3}$$

Our findings, namely the time variation of the width due to the motion of the Earth around the sun holds even when there is an overlap between the two resonances [19].
Since in the axion DM search case the cavity detectors have reached such a very high energy resolution [22,23], one should try to accurately evaluate the width of the expected power spectra in various theoretical models.

3. Evaluation of the width in the local frame

We will derive the expression for the width assuming in the galactic frame a Maxwell Boltzmann axion velocity distribution:

$$f(\upsilon) = \frac{1}{\pi\sqrt{\pi}}\frac{1}{\upsilon_0^3}e^{-\frac{\upsilon^2}{\upsilon_0^2}} \tag{3.4}$$

We will use the relation

$$\omega = m_a\left(1 + \frac{1}{2}\upsilon^2\right) \tag{3.5}$$

or

$$\upsilon = \sqrt{\frac{2(\omega - m_a)}{m_a}}, \upsilon d\upsilon = \frac{d\omega}{m_a}$$

In the galactic frame the number of axions in the with frequency between ω and $\omega + d\omega$ in a solid angle $d\Omega$ is

$$dN_a = \frac{\rho_a}{m_a}\frac{1}{\pi\sqrt{\pi}}\frac{1}{\upsilon_0^3}e^{-2\frac{\omega - m}{m\upsilon_0^2}}\sqrt{\frac{2(\omega - m_a)}{m_a}}\frac{d\omega}{m_a}d\Omega \tag{3.6}$$

Introducing the variable $x = 2\frac{\omega - m_a}{m_a\upsilon_0^2}$ we find:

$$\frac{dN_a}{dx} = \frac{\rho_a}{m_a}g(x)\frac{d\Omega}{4\pi},\ g(x) = \frac{2}{\sqrt{\pi}}e^{-x} \tag{3.7}$$

The maximum of the distribution occurs at $x = 1/2$. The width at half maximum is $\delta x = x_2 - x_1$ with x_i the roots of the equation

$$g(x) = \frac{1}{2}\ g(x)|_{x=1/2} \Rightarrow \sqrt{x}e^{-x} = \frac{1}{2\sqrt{2}}e^{-\frac{1}{2}}$$

We thus find $\delta x = 1.8$. Thus the width at half maximum in frequency space is:

$$\delta\omega = m_a\frac{1}{2}\upsilon_0^2\delta x \Rightarrow \frac{1}{Q_a} = \frac{1}{2}\upsilon_0^2\delta x = \delta x\frac{1}{3} \prec \upsilon^2 \succ_g \tag{3.8}$$

where the last quantity is the average of the square of the axion velocity in the galactic frame.

Our next task is to transform the velocity distribution from the galactic to the local frame. The needed equation, see e.g. [24], is:

$$\mathbf{y} \to \mathbf{y} + \hat{\upsilon}_s + \delta\left(\sin\alpha\hat{x} - \cos\alpha\cos\gamma\hat{y} + \cos\alpha\sin\gamma\hat{\upsilon}_s\right), \quad y = \frac{\upsilon}{\upsilon_0} \tag{3.9}$$

with $\gamma \approx \pi/6$, $\hat{\upsilon}_s$ a unit vector in the Sun's direction of motion, $\hat{x}$ a unit vector radially out of the galaxy in our position and $\hat{y} = \hat{\upsilon}_s \times \hat{x}$. The last term in Eq. (3.9) corresponds to the motion of the Earth around the Sun with δ being the ratio of the modulus of the Earth's velocity around the Sun divided by the Sun's velocity around the center of the Galaxy, i.e. $\upsilon_0 \approx 220$ km/s and $\delta \approx 0.135$. The above formula assumes that the motion of both the Sun around the Galaxy and of the Earth around the Sun are uniformly circular. The exact orbits are, of course, more complicated but such deviations are not expected to significantly modify our results. In Eq. (3.9) α is the phase of the Earth ($\alpha = 0$ around the beginning of June).[2]

[2] One could, of course, make the time dependence of the rates due to the motion of the Earth more explicit by writing $\alpha \approx (6/5)\pi\ (2(t/T) - 1)$, where t/T is the fraction of the year.

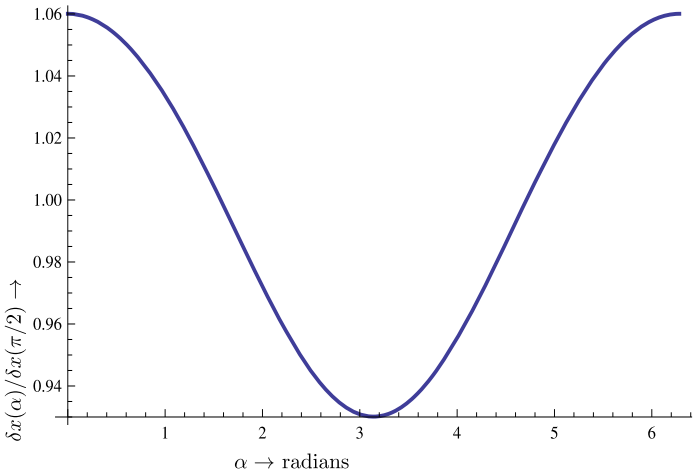

Fig. 3.1. The modulated width δx, relative to its time average, as a function of the phase of the Earth α ($\alpha = 0$ on June 3rd).

We will consider the effect of the Earth's motion in the standard experiments, usually known as modulation effect, which has been recognized as important in axion searches [25]. The azimuthal angle (ϕ) dependence, averages out to zero. Thus the distribution takes the form:

$$\begin{aligned} dN_a &= \frac{\rho_a}{m_a} h(x,\xi,\cos\alpha)\frac{d\Omega}{4\pi},\ h(x,\xi,\cos\alpha) = \frac{2}{\sqrt{\pi}}\sqrt{x}e^{-\left(1+x+(2+\delta\cos\alpha)\xi\sqrt{x}\right)} \\ g(x,\cos\alpha) &= \int h(x,\xi,\cos\alpha)\frac{d\Omega}{4\pi} = \frac{2e^{-x-1}\sinh\left(\sqrt{x}(\delta\cos(\alpha)+2)\right)}{\sqrt{\pi}(\delta\cos(\alpha)+2)} \end{aligned} \tag{3.10}$$

The maximum of the distribution $g(x,\cos\alpha)$ occurs at the root $r_1(\cos\alpha)$ of the equation:

$$\coth\left(\sqrt{x}(\delta\cos(\alpha)+2)\right) - \frac{\sqrt{x}}{\delta\cos(\alpha)+2} = 0$$

which is obtained graphically. Then $\delta x(\cos\alpha) = x_2(\cos\alpha) - x_1(\cos\alpha)$ where $x_1(\cos\alpha)$ and $x_2(\cos\alpha)$ are the roots of the equation:

$$g(x,\cos\alpha) = (1/2)g(r_1(\cos\alpha),\cos\alpha)$$

where

$$g(x,\cos\alpha) = \sqrt{x}e^{-\left(1+x+(2+\delta\cos\alpha)\xi\sqrt{x}\right)}$$

The obtained results are exhibited in Fig. 3.1.

The existing resonators in the axion dark matter search have a quality factor which is more than one order of magnitude larger than the natural axion width. Nonetheless the axion width can be resolved as a narrow line, narrower than the resonator width. This can be accomplished by recording the data with adequate frequency resolution as is currently done by the ADMX and ADMX-HF experiments [9–12]. Even though the cavity width is larger than the axion width the induced electromagnetic field due to axion $\rightarrow$ photon conversion in the presence of the B-field preserves the axion width. The expected width modulation due to the Earth's motion around the sun is roughly $\pm 5\%$, which requires a frequency resolution of better than 1% or better than about 10 Hz for axions at the GHz range. This requirement is well within present technology.

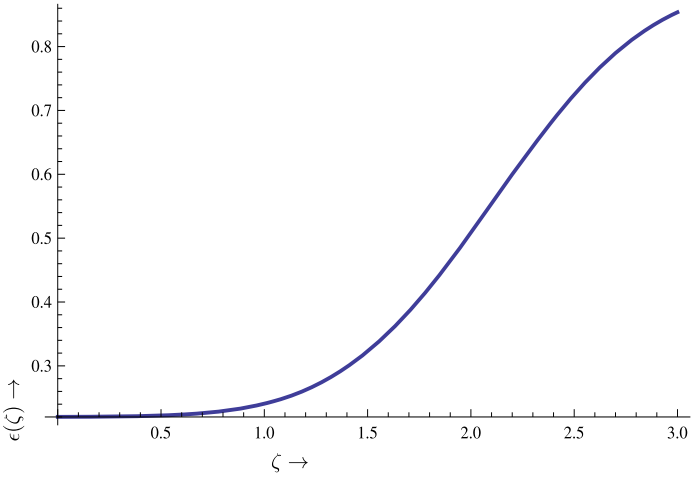

Fig. 4.2. The amplitude $\epsilon(\zeta)$ entering the debris flow component of dark matter. Of particular interest is the region of ζ between 1.5 and 2.

4. More complicated velocity distributions

In the context of dark matter other velocity distributions have also been considered, e.g. completely phase-mixed DM, dubbed "debris flow" (Kuhlen et al. [26]), and caustic rings (Sikivie [27–29], Vergados [30]). We are now going to investigate what is the effect of these distributions on the axion width.

4.1. The case of debris flows

In the case of debris flows one assumes a dark matter distribution which is of the form (see Fig. 4.2):

$$f(\upsilon) = (1 - \epsilon(\zeta)) f_{MB}(\upsilon) + \epsilon(\zeta) f_{db}(\upsilon) \tag{4.11}$$

with

$$f_{db}(\upsilon) = \begin{cases} \frac{1}{2\upsilon_f \upsilon_0}\upsilon, & \upsilon_f - \upsilon_0 \le \upsilon \le \upsilon_f + \upsilon_0 \\ 0 & \text{otherwise} \end{cases} \tag{4.12}$$

where

$$\epsilon(\zeta) = 0.22 + 0.34\left(\text{erf}\left(\zeta\frac{220}{185} - \frac{465}{185}\right) + 1\right) \tag{4.13}$$

The introduction of debris flows has two effects:

- It shifts the maximum of the distribution, without changing the location of the maximum r_1 (see Fig. 4.3).

$$g(x) \rightarrow (1 - \epsilon(\zeta)) g(x) + \epsilon(\zeta) g_{df}(x) \tag{4.14}$$

  with

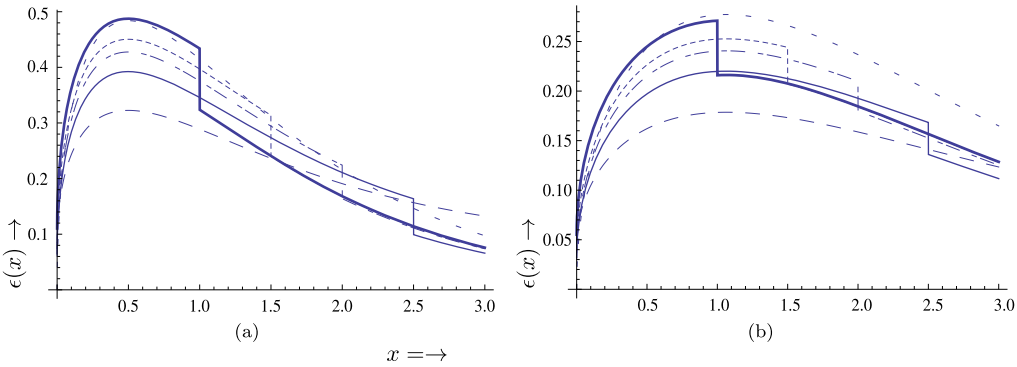

Fig. 4.3. The frequency distribution function $g(x) \rightarrow (1-\epsilon)g(x) + \epsilon g_{df}(x)$ with respect to the galaxy (a) and in the local frame (b). The top line corresponds to $g(x)$ only. Otherwise from top to bottom the lines correspond to $\epsilon = 0.220, 0.222, 0.241, 0.323$ and 0.508.

$$g_{df}(x) = \begin{cases} \frac{1}{4(1+\zeta)}, & \zeta^2 \leq x \leq (2+\zeta)^2 \\ 0 & \text{otherwise} \end{cases} \tag{4.15}$$

- The width at half maximum is affected:

$$g(x) = \frac{1}{2} g(r_1) \Leftrightarrow (1-\epsilon(\zeta))g(x) + \epsilon(\zeta) g_{df}(x) = (1-\epsilon(\zeta))g(r_1) + \epsilon(\zeta) g_{df}(r_1) \tag{4.16}$$

We thus find:

- In the galactic frame:

  $$\delta x = (1.82,\ 1.81,\ 1.97,\ 2.11,\ 2.40) \text{ for } \epsilon = (0.220,\ 0.222,\ 0.241,\ 0.323,\ 0.508)$$

  respectively
- In the local frame:

  $$\delta x = (3.06,\ 3.23,\ 3.28,\ 3.23,\ 2.96) \text{ for } \epsilon = (0.220,\ 0.222,\ 0.241,\ 0.323,\ 0.508)$$

  respectively

The modulation of the width is exhibited in Fig. 4.4.

4.2. The case of caustic rings

Our study of the phase space structure of the Milky Way halo is motivated in large part by the ongoing searches for dark matter on Earth using axion, see e.g. [13,11], and WIMP detectors, see e.g. [31–35]. The signal in such detectors depends on the velocity distribution of dark matter in the solar neighborhood. A search for non-virialized axionic dark matter has been previously considered [36]. The caustic ring halo model predicts, see e.g. [29], that most of the local dark matter is in discrete flows and provides the velocity vectors and densities of the first forty flows at the Earth's location in the Galaxy, which are essential when interpreting a signal in a dark matter detector on Earth. In principle the halo model can be treated as phase-mixed DM leading to a linear combination of a M-B distribution and one appropriate to caustic rings, in a fashion

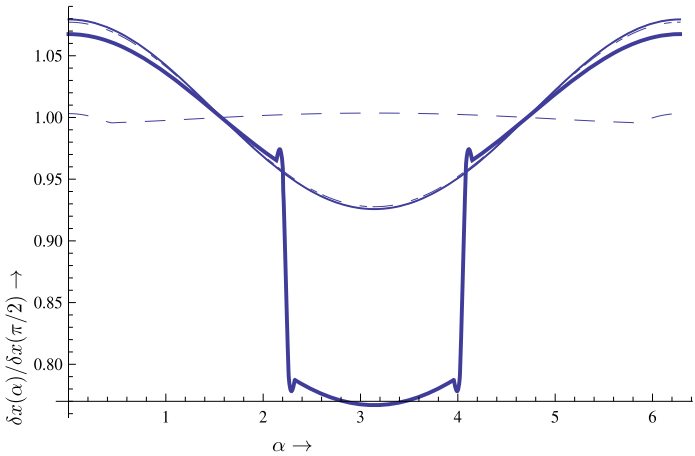

Fig. 4.4. The modulated width, relative to its time average, as a function of the phase of the Earth for various values of ϵ. $\epsilon = 0.220$, 0.222, 0.241, 0.323 0.508 is associated with thick solid, dotted, dot-dashed, fine solid and dashed lines respectively. The dotted and the fine solid lines cannot be resolved.

similar to that with debris flow discussed above. We will, however, concentrate here in caustic rings.

The relevant information for our purposes can be extracted from table V of Duffy and Sikivie [29], which has improved and updated earlier versions, and for the reader's convenience is summarized in Table 4.1. One then writes the velocity distribution as

$$f(\upsilon_z) = \sum_{n\pm} \eta_{\upsilon_\phi^{n\pm}} \delta(\upsilon_z - \upsilon_\phi^{n\pm}),$$
$$f(\upsilon_x) = \sum_{n\pm} \eta_{\upsilon_\rho^{n\pm}} \delta(\upsilon_x - \upsilon_\rho^{n\pm}),$$
$$f(\upsilon_y) = \sum_{n\pm} \eta_{\upsilon_z^{n\pm}} \delta(\upsilon_y - \upsilon_z^{n\pm}) \tag{4.17}$$

where υ_x, υ_y, υ_z are the components of the velocity components in our notation. $\eta_{\upsilon_\phi^{n\pm}}$, $\eta_{\upsilon_\rho^{n\pm}}$, $\eta_{\upsilon_z^{n\pm}}$ are suitable normalization factors extracted from the corresponding densities of the last columns of Table 4.1. With these ingredients we compute the modulated widths, see Fig. 4.5. We observe that the difference between the maximum and the minimum is 0.08. Note, however, that the maximum is shifted from $\alpha = 0$ (June third) $\alpha = 0.079\pi$, i.e. to approximately two weeks later. This is expected due to the asymmetries in the caustic velocity distribution.

5. Discussion

In the present work we studied possible effects on the width of the axion to photon resonance cavities involved in Axion Dark Matter Searches, by considering a number of popular halo models. We also examined the annual variation of the width due to the motion of the Earth around the sun. The relative width, i.e. the width divided by its time average, can attain significant differences between the maximum expected in June and the minimum expected six months later. This variation is larger than the modulation expected in ordinary dark matter searches of WIMPs. It does not depend on the geometry of the cavity or other details of the apparatus. It

Table 4.1
The velocities caustic ring velocities in our vicinity of our galaxy. The components are given in Sikivie's notation. In our notation for the galactic axes we use $\hat{\phi} \to \hat{z}, \hat{\rho} \to \hat{x}, \hat{z} \to \hat{y}$.

n	$\upsilon^{n\pm}$ km/s	$\upsilon_\phi^{n\pm}$ km/s	$\upsilon_z^{n\pm}$ km/s	$\upsilon_\rho^{n\pm}$ km/s	d_n^+ 10^{-26} gr/cm^3	d_n^- 10^{-26} gr/cm^3
1	650	140	±635	0	0.3	0.3
2	600	250	±540	0	0.8	0.8
3	565	380	±420	0	1.9	1.9
4	540	440	±310	0	3.4	3.4
5	520	505	0	±120	150.	15.
6	500	430	0	±260	6.0	3.1
7	490	360	0	±330	3.9	1.2
8	475	325	0	±350	1.9	1.0
9	460	265	0	±375	1.4	0.7
10	450	220	0	±390	0.9	0.9
11	440	200	0	±390	0.8	0.8
12	430	180	0	±390	0.7	0.7
13	420	170	0	±390	0.6	0.6
14	415	155	0	±385	0.6	0.6
15	405	140	0	±380	0.5	0.5
16	400	13	0	±375	0.5	0.5
17	390	120	0	±370	0.5	0.5
18	380	110	0	±365	0.4	0.4
19	375	100	0	±360	0.4	0.4
20	370	95	0	±355	0.4	0.4

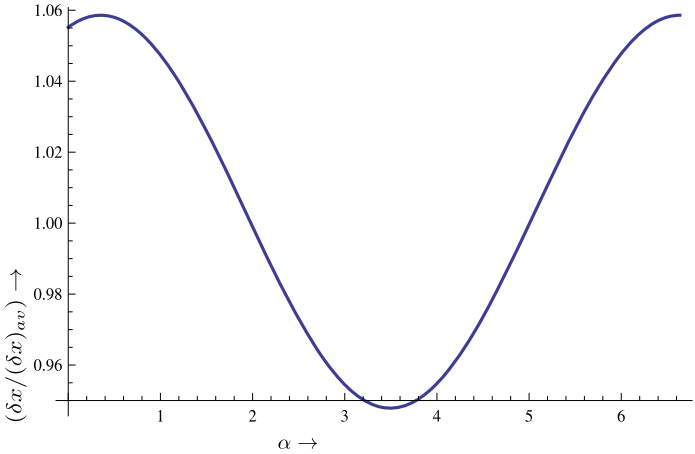

Fig. 4.5. The width modulated width δx relative to the time averaged width expected in the case of caustic rings. Note that in this case the maximum does not occur at $\alpha = 0$, but a bit later.

only depends on the assumed velocity distribution. Furthermore the predicted time variation of the width (modulation) is observable with the present technology.

In conclusion in this work we have elaborated on signatures that might aid the analysis of axion dark matter searches. Eventually, if such an observation is made, one may be able to exploit the results obtained here to gain information about the velocity distribution associated with the various halo models.

Acknowledgements

J.D.V. acknowledges that this work was supported by Project Code IBS-R017-D1-2016-a00 in the Republic of Korea and by the ARC Centre of Excellence in Particle Physics (CoEPP), University of Adelaide, Australia. He is indebted to Professor A. Thomas for support and hospitality.

References

[1] R. Peccei, H. Quinn, Phys. Rev. Lett. 38 (1977) 1440.
[2] S. Weinberg, Phys. Rev. Lett. 40 (1978) 223.
[3] F. Wilczek, Phys. Rev. Lett. 40 (1978) 279.
[4] J. Preskill, M.B. Wise, F. Wilczek, Phys. Lett. B 120 (1983) 127.
[5] L.F. Abbott, P. Sikivie, Phys. Lett. B 120 (1983) 133.
[6] M. Dine, W. Fischler, Phys. Lett. B 120 (1983) 137.
[7] J. Primack, D. Seckel, B. Sadoulet, Annu. Rev. Nucl. Part. Sci. 38 (1988) 751.
[8] P. Sikivie, Phys. Rev. Lett. 51 (1983) 1415.
[9] I.P. Stern, Physics.ins–det, on behalf of ADMX and ADMX-HF collaborations, Axion dark matter searches, arXiv:1403.5332, 2014.
[10] G. Rybka, The axion dark matter experiment, IBS MultiDark Joint Focus Program WIMPs and Axions, Daejeon, S. Korea, October 2014.
[11] S.J. Asztalos, et al., Phys. Rev. Lett. 104 (2010) 041301, the ADMX Collaboration, arXiv:0910.5914 [astro-ph.CO].
[12] A. Wagner, et al., Phys. Rev. Lett. 105 (2010) 171801, for the ADMX Collaboration; arXiv:1007.3766.
[13] S.J. Asztalos, et al., Nucl. Instrum. Methods Phys. Res., Sect. A, Accel. Spectrom. Detect. Assoc. Equip. 656 (2011) 39, arXiv:1105.4203 [physics.ins-det].
[14] Center for Axion and Precision Physics research (CAPP), Daejeon 305-701, Republic of Korea, More information is available at http://capp.ibs.re.kr/html/capp_en/.
[15] G. Raffelt, Astrophysical axion bounds, IBS MultiDark Joint Focus Program WIMPs and Axions, Daejeon, S. Korea, October 2014.
[16] Y. Semertzidis, J.D. Vergados, Nucl. Phys. B 897 (2015) 821, arXiv:1412.6907.
[17] Y. Semertzidis, J.D. Vergados, in: Proceedings of the 18th International Conference: From the Planck Scale to the Electroweak Scale, 25–29 May 2015 Ioannina, Greece, arXiv:1511.08516.
[18] Y.H. Ahn, Flavored Peccei–Quinn symmetry, arXiv:1410.1634 [hep-pj].
[19] J. Hong, J.E. Kim, S. Nam, Y. Semertzidis, Physics.ins–det, calculations of resonance enhancement factor in axion-search tube experiments, arXiv:1403.1576, 2014.
[20] J.E. Kim, Phys. Rev. D 58 (1998) 055006.
[21] L. Krauss, J. Moody, F. Wilczek, D. Morris, Phys. Rev. Lett. 55 (1985) 1797.
[22] L. Duffy, et al., Phys. Rev. Lett. 95 (2005) 09134, for the ADMX Collaboration.
[23] L. Duffy, et al., Phys. Rev. D 74 (2006) 012006, for the ADMX Collaboration.
[24] J. Vergados, Phys. Rev. D, Part. Fields 85 (2012) 123502, arXiv:1202.3105.
[25] http://www.slac.stanford.edu/econf/C040802/papers/MOT002.PDF, 2004, SLAC Summer Institute on Particle Physics (SSI04), Aug. 2–13, 2004.
[26] M. Kuhlen, M. Lisanti, D. Speregel, Phys. Rev. D 86 (2012) 063505, arXiv:1202.0007 [astro-ph.GA].
[27] P. Sikivie, Phys. Rev. D 60 (1999) 063501.
[28] P. Sikivie, Phys. Lett. B 432 (1998) 139.
[29] L.D. Duffy, P. Sikivie, Phys. Rev. D 78 (2008) 063508.
[30] J.D. Vergados, Phys. Rev. D 63 (2001) 063511.
[31] E. Aprile, et al., Phys. Rev. Lett. 107 (2011) 131302, arXiv:1104.2549v3 [astro-ph.CO].
[32] R. Bernabei, et al., Int. J. Mod. Phys. A 28 (2013) 1330022, http://dx.doi.org/10.1142/S0217751X13300226.
[33] E. Armengaud, et al., Phys. Lett. B 702 (2011) 329, arXiv:1103.4070v3 [astro-ph.CO].
[34] D. Akerib, et al., Phys. Rev. Lett. 96 (2006) 011302, arXiv:astro-ph/0509259.
[35] K. Abe, et al., Astropart. Phys. 31 (2009) 290, arXiv:0809.4413v3 [physics.ins-det].
[36] J. Hoskins, et al., Phys. Rev. D 84 (2011) 121302, arXiv:1109.4128 [astro-ph.CO].